# Ultra-high Resolution True FISP Projection Reconstruction Imaging for Cardiac Function Evaluation

Dana C. Peters, Elliot R. McVeigh,
Laboratory of Cardiac Energetics, National Heart, Lung and Blood Institute, Bethesda Maryland, 20892 USA

## INTRODUCTION

The high achievable spatial resolution of undersampled projection reconstruction (PR) (1) is combined with the excellent contrast and signal-to-noise ratio of true FISP imaging (2) for cardiac function evaluation (PR FISP). The results are movies of cardiac function with higher resolution than previously reported (3). These movies reveal interesting trabecular and papillary structures on the endocardium (Fig. 1).

Diagnostic imaging of the myocardium focuses on its function and contractility (cardiac function imaging, and tagging) or its uptake of contrast (perfusion and hyperenhancement imaging). Visualization of the endocardium is important, because ischemia and infarction commonly occur is this region. What are the implications of the fine trabecular structure of the endocardium for low-resolution imaging? Here is presented an initial investigation of the importance of fine endocardial structures on cardiac imaging. The papillary and trabecular fraction of the myocardium is quantified. The influence of trabecular myocardium on MRI wall strain measurements is demonstrated.
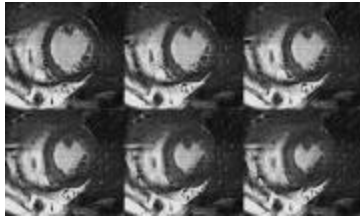


**Figure 1:** PR FISP short-axis images with 0.8 x 0.8 mm resolution. A sequence of time-frames (32 ms temporal resolution) from begin-systole to end-systole is shown for a single slice. Note the appearance of papillaries and trabeculae on the endocardium.

In order to obtain and evaluate heart images with 800 x 800 micron resolution and high SNR, a 400 x 256 Np PR acquisition was chosen for this study. This resulted in a long 32 second breath-hold, to obtain 32 ms temporal resolution. Greater undersampling would provide shorter breath-holds. Potentially, high resolution PR FISP with greater undersampling could be used to image important high resolution features of the heart within a short breath-hold.

## METHODS

Figure 2 shows the 2D pulse sequence diagram. The data was collected in fractional gradient echoes. The excitation pulse was a truncated sinc pulse, and the slice-select gradient rephaser was played simultaneously with the readout-gradient rephasers. In accordance with the pulse sequence requirements for creating a true FISP state, each TR is 0th-order gradient moment nulled, and 180? phase cycling is applied to the excitation pulse [4]. In some situations, 1st gradient moment nulling was also used for Gx, Gy and Gz. The sequence was implemented on a GE 1.5 T CV/i scanner, equipped with 4 G/cm maximum gradient strengths, and 150 T/m/s slew-rates. Typical scan parameters (without 1st moment nulling) were: TR/TE/flip = 4.4 ms/1.4ms/60º, field of view = 32 cm, 8 mm slices, readout resolution of 400, 256 projections, +/-125 kHz bandwidth, cardiac phased-array coil. The raw data was reconstructed offline using a regridding algorithm and 2D Fourier transform. Segmented ecg-gated acquisitions (8 views per segment) in a 32 heart-beat breath-hold provided a temporal resolution of about 32 ms. The in-plane spatial resolution was 800 x 800 microns.
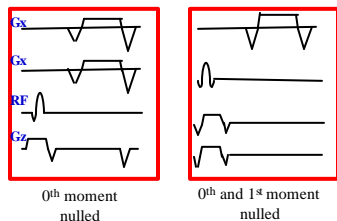


Figure 2. A 2D projection reconstruction true FISP sequence with 0th moment nulling. Alternatively, a 0th and 1st moment nulled sequence was used.

0th moment nulled

0th and 1st moment nulled

## METHODS (cont.)

The trabecular fraction of the myocardium was quantified for 16 sectors around the myocardium at end-diastole. Three contours were manually drawn, as shown in Fig. 3: the endocardial border including the papillaries and trabeculae, the endocardial border excluding papillaries and trabeculae, and the epicardial border. The trabecular fraction was defined as the ratio of the area of trabeculation to the total myocardial area, approximately: $(R_{endo}^2 R_{trab}^2)/(R_{epi}^2 R_{trab}^2)$. Myocardial wall strain measurements were performed to investigate the strain in regions of known trabeculation. A 2D strain analysis was performed using FindTags (5) on tagged images with PR FISP comparison images.
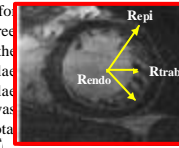


**Figure 3** The trabecular fraction of myocardium was determined as the portion of the myocardium which is a mixture of blood and myocardium.

## RESULTS

### High resolution PR FISP vs. conventional cardiac function imaging



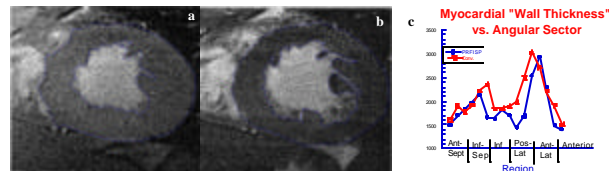**Myocardial "Wall Thickness" vs. Angular Sector**

**Figure 4 compares a frame at begin-systole from (a) a conventional cine movie (1.2 x 2.5 x 8mm) and (b) a high resolution true FISP movie (0.8 x 0.8 x 8mm).** The manually contoured endocardial and epicardial borders are shown in blue. Figure 4c compares the calculated myocardial "wall thickness" (the myocardial area within a sector) for each image. The myocardial wall measurements agree well, except for regions where there is a mixture of blood and myocardium (e.g. the posterior-lateral wall). Additionally, the high resolution PR FISP images reveal that much of this myocardium is trabecular and papillary.
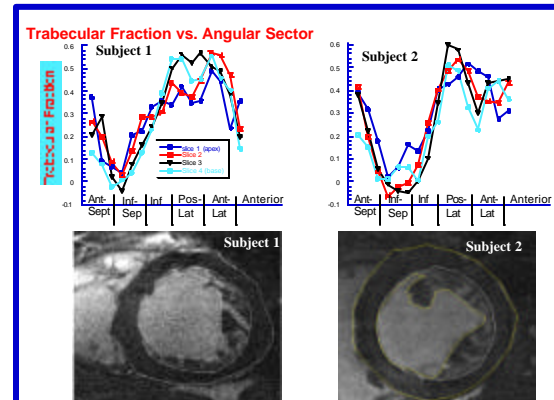


**Trabecular Fraction vs. Angular Sector**

Subject 1

Subject 2

**Figure 5:** The results of quantifying the trabecular fraction of myocardium for two volunteers in four short-axis slices. The graphs show the fraction of myocardium which is trabecular for sectors of the myocardium at end-diastole. Representative images and contours from both volunteers are shown. The contours show the trabecular, endocardial and epicardial traces. As much as 60% of the myocardial wall thickness is trabecular.

## RESULTS (cont.)

Figure 5 shows the results of quantifying trabecular fraction in two volunteers. For each volunteer, the fraction in four short axis slices was determined, measured at begin-systole. Representative images and contours from both volunteers are shown. The contours show the trabecular, endocardial and epicardial traces. As much as 60% of the myocardial wall thickness is trabecular.

### Myocardial Tagging of Trabeculae and Papillaries.

Using the techniques of myocardial wall tagging with MR, many investigators have reported increased strain measurements on the anterior-lateral wall (the free wall) compared to the septum, with higher strains ranging from 20% to 40% (5,6). These investigators have also measured transmural strain gradients and reported increased strain on the endocardium compared to the epicardium. To investigate the influence of trabecular and papillary structures on tagging strain measurements, tagged and high resolution PR FISP images were obtained for the same slice. Figure 6 compares a tagged image (6a) and a high resolution PR FISP image (6b) of the same slice and time frame. The circumferential shortening map (Ecc) was determined using the tagged data set and contours drawn from the tagged images, and is shown at end-systole in Fig. 6c. The free wall is highly trabeculated, and the high strain values on the free wall reflect this as apparent increased contractility.
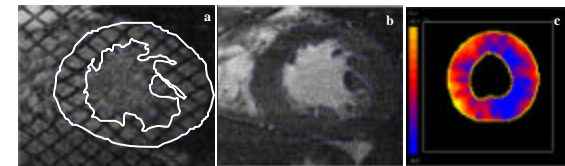


Figure 6: A tagged MR image(a), and a high-resolution PR FISP (b) image of the same slice and phase in the cardiac cycle. The contours of the FISP image are superimposed onto the tagged image. The tagged data set was used to calculate circumferential shortening, showing increased shortening in regions of trabeculation at end-systole (c).

## CONCLUSIONS

• High resolution PR FISP reveals fine trabecular and papillary structure previously only observed in isolated hearts. This is due to the excellent contrast of FISP, and the high resolution achievable with PR.

• As much as 60% of the left ventricular wall, as seen in the MR images, is actually a border zone containing myocardial trabeculae and blood (in some angular sectors).

• Myocardial strain measurements of the left ventricle which report higher strain values on the free wall than the septum are influenced by the less constrained motion of the trabecular myocardium.

• In this study, only moderate undersampling was employed to maintain high SNR. Greater undersampling might allow high resolution imaging in shorter breath-holds, potentially for imaging important high-resolution features of the heart in patients.

## REFERENCES

1. Peters et al., MRM. 43(1): 91-101(2000). 2. O. Heid, ISMRM 1997, 320. 3. J Carr et al., ISMRM 2000 199. 4. JL Duerck et al., JMRI 8 203-208 (1998). 5. MA Guttman, IEEE Computer Graphics, 30-38 (1997). 6. ER McVeigh, MRI 14(2):147 (1996). 7. CC Moore et al. Radiology 214(2):453-466 (2000).